

Molded transparent photopolymers and phase shift optics for fabricating three dimensional nanostructures

Seokwoo Jeon¹, Daniel J. Shir¹, Yun Suk Nam¹, Robert Nidetz¹, Matthew Highland¹,
David G. Cahill¹, John A. Rogers*¹, Mehmet F. Su², Ihab F. El-Kady^{2,3},
Christos G. Christodoulou², and Gregory R. Bogart³

¹ Department of Materials Science and Engineering, Electrical and Computer Engineering, and Chemistry, Beckman Institute and Seitz Materials Research Laboratory, University of Illinois, Urbana, IL 61801

² Department of Electrical and Computer Engineering, University of New Mexico, Albuquerque, NM 87131

³ Sandia National Laboratory, Albuquerque, NM 87185

*Corresponding author: jrogers@uiuc.edu

Abstract: This paper introduces approaches that combine micro/nanomolding, or nanoimprinting, techniques with proximity optical phase mask lithographic methods to form three dimensional (3D) nanostructures in thick, transparent layers of photopolymers. The results demonstrate three strategies of this type, where molded relief structures in these photopolymers represent (i) fine (<1 μm) features that serve as the phase masks for their own exposure, (ii) coarse features (>1 μm) that are used with phase masks to provide access to large structure dimensions, and (iii) fine structures that are used together phase masks to achieve large, multilevel phase modulations. Several examples are provided, together with optical modeling of the fabrication process and the transmission properties of certain of the fabricated structures. These approaches provide capabilities in 3D fabrication that complement those of other techniques, with potential applications in photonics, microfluidics, drug delivery and other areas.

© 2007 Optical Society of America

OCIS codes: (220.4000) Microstructure fabrication; (320.7110) Ultrafast nonlinear optics; (050.0050) Diffraction and gratings

References and links

1. P. J. A. Kenis, R. F. Ismagilov, and G. M. Whitesides, "Microfabrication inside capillaries using multiphase laminar flow patterning," *Science* **285**, 83-85 (1999).
2. Y. N. Xia and G. M. Whitesides, "Soft lithography," *Angew. Chem., Int. Ed. Engl.* **37**, 551-575 (1998).
3. D. G. Grier, "A revolution in optical manipulation," *Nature* **424**, 810-816 (2003).
4. D. N. Christodoulides, F. Lederer, and Y. Silberberg, "Discretizing light behavior in linear and nonlinear waveguide lattices," *Nature* **424**, 817-823 (2003).
5. J. H. Holtz and S. A. Asher, "Polymerized colloidal crystal hydrogel films as intelligent chemical sensing materials," *Nature* **389**, 829-832 (1997).
6. J. W. Long, B. Dunn, D. R. Rolison, and H. S. White, "Three-Dimensional Battery Architectures," *Chem. Rev.* **104**, 4463-4492 (2004).
7. B. T. Holland, C. Blanford, and A. Stein, "Synthesis of macroporous minerals with highly ordered three-dimensional arrays of spheroidal voids," *Science* **281**, 538-540 (1998).
8. B. H. Cumpston, S. P. Ananthavel, S. Barlow, D. L. Dyer, J. E. Ehrlich, L. L. Erskine, A. A. Heikal, S. M. Kuebler, I. Y. S. Lee, D. McCord-Maughon, J. Qin, H. Rockel, M. Rumi, X.-L. Wu, S. R. Marder, and J. W. Perry, "Two-photon polymerization initiators for three-dimensional optical data storage and microfabrication," *Nature* **398**, 51-54 (1999).
9. S. Uemura, "The activities of FGM on new application," *Mater. Sci. Forum* **423-425**(Functionally Graded Materials VII), 1-10 (2003).
10. B. Kaehr and J. B. Shear, "Mask-Directed Multiphoton Lithography," *J. Am. Chem. Soc.* **129** 1904-1905 (2007).
11. D. B. Shao and S. C. Chen, "Direct patterning of three-dimensional periodic nanostructures by surface-plasmon-assisted nanolithography," *Nano. Lett.* **6**, 2279-2283 (2006).

12. S. Jeon, V. Malyarchuk, J. O. White, and J. A. Rogers, "Optically fabricated three dimensional nanofluidic mixers for microfluidic devices," *Nano. Lett.* **5**, 1351-1356 (2005).
 13. S. Jeon, J.-U. Park, R. Cirelli, S. Yang, C. E. Heitzman, P. V. Braun, P. J. A. Kenis, and J. A. Rogers, "Fabricating complex three-dimensional nanostructures with high-resolution conformable phase masks," *Proc. Natl. Acad. Sci. U. S. A.* **101**, 12428-12433 (2004).
 14. W. Zhou, Y. Huang, E. Menard, N. R. Aluru, J. A. Rogers, and A. G. Alleyne, "Mechanism for stamp collapse in soft lithography," *Appl. Phys. Lett.* **87** 251925 (2005).
 15. K. J. Hsia, Y. Huang, E. Menard, J. U. Park, W. Zhou, J. Rogers, and J. M. Fulton, "Collapse of stamps for soft lithography due to interfacial adhesion," *Appl. Phys. Lett.* **86**, 154106 (2005).
 16. S. Jeon, Y. Nam, D. Shir, J. Rogers, and A. Hamza, "three dimensional nanoporous density graded materials formed by optical exposures through conformable phase masks'," *Appl. Phys. Lett.* **89**, 253101 (2006).
 17. S. Jeon, V. Malyarchuk, J. A. Rogers, and G. P. Wiederrecht, "Fabricating three dimensional nanostructures using two photon lithography in a single exposure step," *Opt. Express* **14**, 2300-2308 (2006).
 18. K. E. Paul, T. L. Breen, J. Aizenberg, and G. M. Whitesides, "Maskless photolithography: Embossed photoresist as its own optical element," *Appl. Phys. Lett.* **73**, 2893-2895 (1998).
 19. K. E. Paul, T. L. Breen, T. Hadzik, G. M. Whitesides, S. P. Smith, and M. Prentiss, "Imaging patterns of intensity in topographically directed photolithography," *J. Vac. Sci. Technol. B* **23**, 918-925 (2005).
 20. F. Hua, Y. G. Sun, A. Gaur, M. A. Meitl, L. Bilhaut, L. Rotkina, J. F. Wang, P. Geil, M. Shim, J. A. Rogers, and A. Shim, "Polymer imprint lithography with molecular-scale resolution," *Nano. Lett.* **4**, 2467-2471 (2004).
 21. "The GSOLVER ver. 4.20 developed by Grating Solver Development Company (P.O. Box 353, Allen, TX 75013)."
 22. H. Tan, A. Gilbertson, and S. Y. Chou, "Roller nanoimprint lithography," *J. Vac. Sci. Technol. B* **16**, 3926-3928 (1998).
 23. L. F. Li, "Formulation and comparison of two recursive matrix algorithms for modeling layered diffraction gratings," *J. Opt. Soc. Am. A* **13**, 1024-1035 (1996).
-

1. Introduction

Applications of three dimensional (3D) nanostructures in microfluidics, [1, 2] photonics, [3, 4] sensors, [5] fuel cells and battery devices, [6] catalyst supports, [7] data storage materials, [8] and density gradient systems [9] create interest in the development of methods for fabricating such structures. Many techniques exist, although most have disadvantages, including some combination of slow patterning speeds, limited structure geometries, experimentally inconvenient setups, and difficult scale-up to large areas. Methods that use three dimensional optical techniques with phase and/or amplitude masking elements that are relatively simple to use, they can involve parallel, high speed (i.e. single exposure) operation and they can be applied to large areas [10, 11]. One such method, which we refer to as proximity field nanoPatterning (PnP), [12, 13] uses conformable, elastomeric phase masks to pattern thick, transparent layers of photosensitive materials. This approach involves a contact exposure geometry achieved through the action of generalized adhesion forces that pull the mask into atomic-scale, conformal contact with the photosensitive layer [14, 15]. Light passing through the mask creates a three dimensional distribution of intensity in proximity to its surface that exposes the photosensitive layer through its thickness [13]. Removing the regions of material that have (or have not, depending on the chemistry) been exposed yields a solid form, 3D replica of the intensity distribution. The optics of this system, which involves self-imaging and Talbot effects, determines the geometries of these 3D structures. The layout of the mask and its optical properties, the coherence, wavelength and directionality of the exposure light, the optical properties of the photosensitive material and the nature of its interaction with the exposure light (e.g. one or multi photon effects) represent some of the parameters that can be controlled to yield structures with certain desired 3D shapes. Although many varied classes of periodic and aperiodic 3D structures have been demonstrated [12, 13, 16, 17], important limitations remain.

This paper presents methods that extend the range of structures that can be formed by PnP and related approaches. The results introduce, in particular, methods for using molding, or nanoimprinting, techniques to form patterns of relief in photosensitive materials that can be used in combination with, or as replacements for, the masking optics. This strategy provides important additional flexibility in the patterning process that can be exploited to yield 3D structures with potential applications in photonics and other areas. In one version of this

approach, fine surface relief features (i.e. sub-micron) molded on a transparent photosensitive material provide a phase modulation that acts, effectively, as a phase mask for patterning the optical exposure of this material under uniform illumination. This use of molded relief as a phase mask is conceptually related to previous demonstrations of patterning two dimensional thin (~ 100 nm) line structures using near field effects [18, 19]. The 3D implementation introduced here, which we refer to as maskless PnP, is important because it provides access to phase mask characteristics (i.e. depths of phase modulation and feature sizes), and resulting structure geometries that are difficult to achieve using known materials for the elastomeric phase masks used in the usual version of PnP. A second variant of this molding approach, which is conceptually different than the first, uses comparatively coarse molded features of relief with optical exposures through separate phase mask elements. 3D structures with both fine (i.e. 100 nm – 5 μ m) and coarse (i.e. 10 μ m to several centimeters or larger) features can be achieved in this manner. In a third embodiment, molded and separate phase masks are implemented together to yield large, multiple levels of phase modulation from shallow, binary relief in the masks, thereby providing an experimental route to 3D log pile and other structures that are difficult to form with simple masks in a single exposure step. These three approaches, which all rely on the concept of the combined use of molding and phase mask techniques, are illustrated in the following through optical modeling and the fabrication of representative structures.

2. Experimental

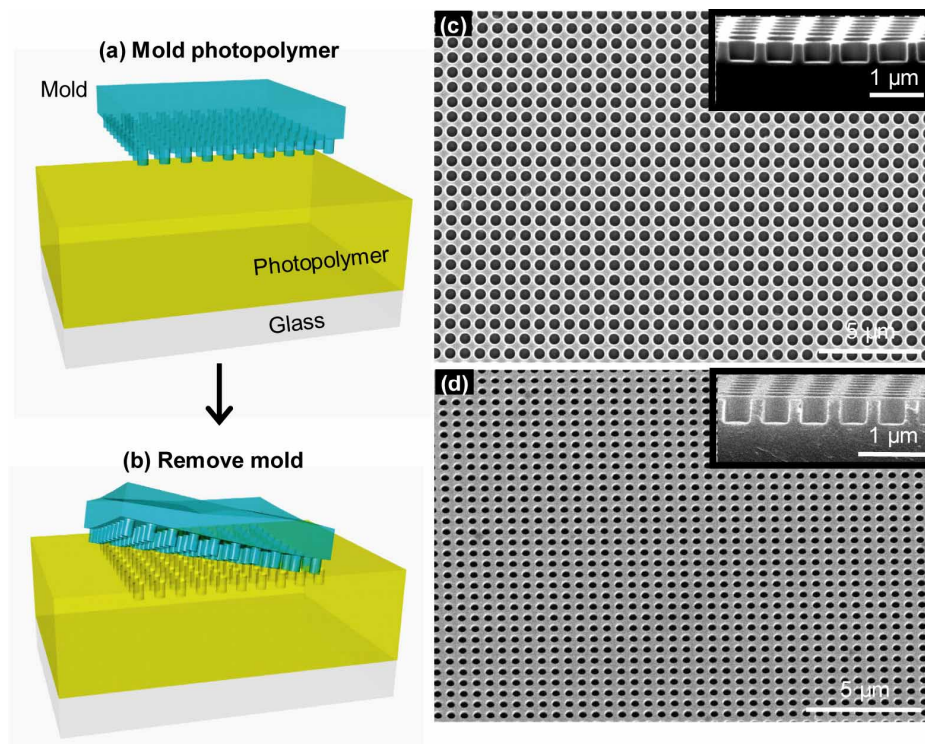


Fig. 1. Schematic illustration of the formation of relief structures on the surface of a photosensitive transparent polymer (SU-8) (a, b) for a maskless, phase optic approach to formation of 3D nanostructures. Scanning electron micrographs of the molded structures (c, d). These relief patterns consist of square arrays of cylindrical holes (depth: 420 nm) with diameters of 570 nm (c, mask 1) and 375 nm (d, mask 2) and periodicities of 710 nm and 566 nm, respectively. Highly uniform structures of this type can be formed over large areas (5×5 mm for the examples shown here).

Figure 1 shows the basic molding approach, as implemented for the case that the molded relief provides the phase modulation for 3D patterning. For the work described here, the molds consisted of surface embossed pieces of the elastomer poly(dimethylsiloxane) (PDMS, Dow Corning), formed using the casting and curing processes of soft lithography with patterns of photoresist on silicon wafers as templates. The fabrication details can be found elsewhere [10,19]. The relief structures consisted of parallel lines and cylindrical posts in square arrays. The latter masks involved diagonal dimensions (d), heights (h) and center to center separations (p) of $d=570$ nm, $h=420$ nm, and $p=710$ nm for ‘mask 1’, and $d=375$ nm, $h=420$ nm, and $p=566$ nm for ‘mask 2’. The former masks, which we refer to as ‘mask 3’ and ‘mask 4’, consisted of line and space gratings with $h=220$ nm and $p=400$ nm and $h=10$ μ m and $p=20$ μ m, respectively. Thick (~ 10 μ m), spin-coated (3000 rpm, 30 sec) layers of an epoxy based negative photoresist (SU-8, Microchem) served as the photosensitive material. The PDMS molds created surface relief structures in these layers in solvent assisted (ethanol) or thermal (~ 75 C) nanoimprinting processes [2]. Highly reproducible, spatially uniform structures of surface relief over areas limited only by the size of the PDMS elements (5 x 5 mm for results presented here) and with dimensions down to the single nanometer range can be achieved with these procedures [20]. Figure 1 provides scanning electron micrographs of some representative structures obtained with mask 1 and mask 2. The exposure step consisted of passing a uniform beam of laser light through the molded samples such as these, with or without a PDMS phase mask in contact with their surfaces. These exposures exploited one and two photon effects (1-ph and 2-ph, respectively) in the SU8. For the one photon (1-ph) case, the central part (~ 6 mm in diameter) of the collimated, linearly polarized 355 nm output of a tripled Nd:YAG laser (Teem Photonics Inc.) was used. The laser had pulse duration of 0.46 ns at a repetition rate of 9.12 KHz and average power of 6.8 mW. A regeneratively amplified Ti:Sapphire laser (Spectra-Physics, Spitfire Pro) operating at a wavelength of 800 nm with an energy/pulse of ~ 1.80 mJ, a repetition rate of 1 KHz, and a pulse width of ~ 140 fs provided the high intensity exposure source for two photon patterning. Circularly polarized light was used in this case [17]. A single lens with a focal length of $f = 400$ mm focused the beam to provide the necessary intensity (~ 1 TW/cm²) for effective two photon exposure. Even though the beam was not fully collimated, its small convergence angle (< 10 mrad) led to minimal effects in the patterned structures. This non-collimated setup allowed the intensity at the sample to be adjusted simply by translating the sample. The diameter of the beam out of the laser was ~ 1 cm; the diameter at the exposure location was 3-4 mm. In both the one and two photon cases, postexposure baking of the SU8, followed by washing away the uncrosslinked regions and supercritical drying completed the fabrication [10]. Optical modeling used a commercial rigorous coupled wave analysis package (gsolver [21]) and a separate interference code written in Matlab (Mathworks Inc.). Details can be found elsewhere [13, 17].

3. Results and discussions

Figure 2 presents structures formed by passing 355 nm laser light through the structures of Fig. 1, in a 1-ph maskless PnP process. Mask 1 and mask 2 formed the relief structures for Figs. 2(b), 2(c) and Figs. 2(d), 2(e), respectively. Calculation shows that the numbers of beams diffracted by the molded relief, which determine the number of spatial Fourier components associated with the structures, are 37 and 21 for Mask 1 and 2, respectively. The associated differences in the structures are qualitatively apparent from the cross-sectional images [Figs. 2(b), 2(e)]. The overall geometries in these two cases each resemble those formed by exposure of flat layers of SU8 with these masks [13] because the number of diffraction orders and their propagation vectors are similar in the mask and maskless cases. Some differences appear in the surface regions, due to the molded relief and the prominence of near field effects. Other, more subtle, differences in the bulk of the patterned structures are also present, due to differences in the index of refraction of PDMS and SU8 and in the coupling of diffracted light into the bulk of the SU8 films. The results suggest, then, that in the regime where the phase structures create many diffracted beams, maskless PnP can

provide an alternative route of patterning when direct conformal contact of phase mask to patterning material is not feasible. Also, the molding process can be implemented in ways that are inconvenient with masks. For example, molding with a small mold in a step-and-repeat fashion or with a cylindrical mold in a continuous reel-to-reel setup [22] can yield processed films that are suitable for large area maskless patterning in a single exposure step.

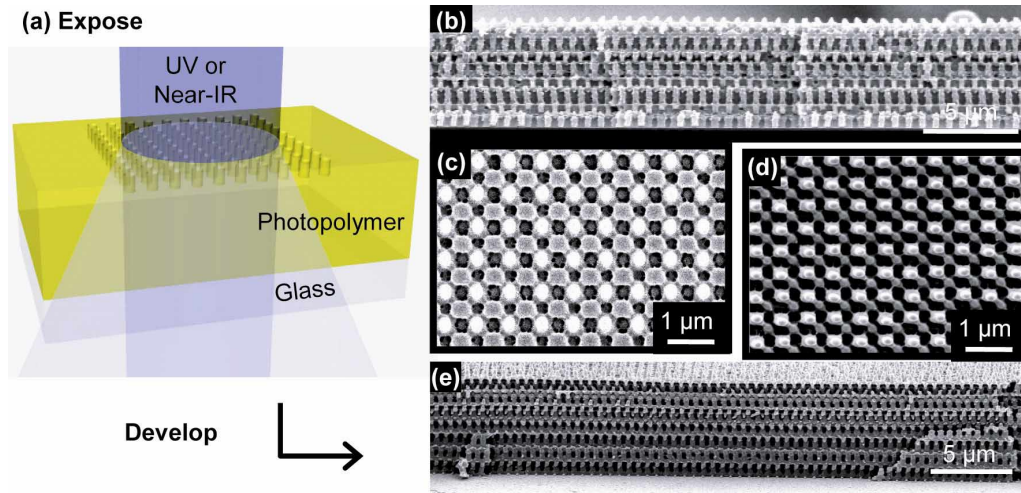


Fig. 2. Schematic illustration (a) of optical exposure through the molded surface of a transparent layer of a photopolymer (SU-8). Cross-sectional (b, e) and top view (c, d) scanning electron micrographs of 3D nanostructures by developing away unexposed regions of the polymer. Mask 1 and 2 were used for (b, c) and (d, e), respectively.

The value of the maskless approach in producing structure geometries that are not easily achieved using the mask based technique is most clearly evident when applied in a 2-ph patterning mode. Previous work [17] reported body centered tetragonal structures produced by 2-ph PnP with 810 nm fs pulsed exposure light and a phase mask with $h=510$ nm, $d=570$ nm and $p=710$ nm. Similar structures with face centered cubic geometries would require a mask with a much shorter period, $p \sim 540$ nm. The fabrication challenges associated with creating an elastomeric mask that has this geometry and, at the same time, offers sufficient depth of relief to provide adequate phase shifting are extreme. Mechanical instabilities and fracture of relief features in typical elastomers make sub-micron features with aspect ratios of larger than $\sim 2\times$ are difficult to produce reliably. Classes of elastomers (e.g. PDMS or perfluoropolyether) that have been used for phase masks have indices of refraction in the range of 1.34-1.4. These two considerations lead to masks with the lateral layout of mask 2, for example, that can provide, at most, phase shifts of up to $\sim 0.5\pi$. Mask 2 offers such a small phase modulation (i.e. $\sim 0.4\pi$) that the intensity contrast (I_{\max}/I_{\min}) of the 3D intensity distribution that forms in the photoresist with 800 nm light is only <6 , even in 2-ph mode.

The maskless approach avoids this problem because it transfers relief structure from the elastomeric masks into the photosensitive materials, which can be designed with comparatively high index of refraction. The index of SU8 is, for example, ~ 1.58 . This value leads to a phase modulation of $\sim 0.63\pi$ and an intensity contrast of >50 in the same 2-ph mode. Figure 3 presents a representative 3D patterning result, together with optical modeling of the intensity distribution. This structure has close to face centered cubic (FCC) symmetry, with lattice parameters of 800 nm in-plane [Fig. 3(c)] and 915 nm out-of-plane [Fig. 3(d)], both in good agreement with modeling. These types of layouts might have possible applications and wavelength selective filters and, if used as templates for the growth of high index materials, as photonic bandgap structures. The bottom frame of Fig. 3 illustrates some measurements and calculations of transmission of light passing through a representative structure in a direction parallel to its surface normal.

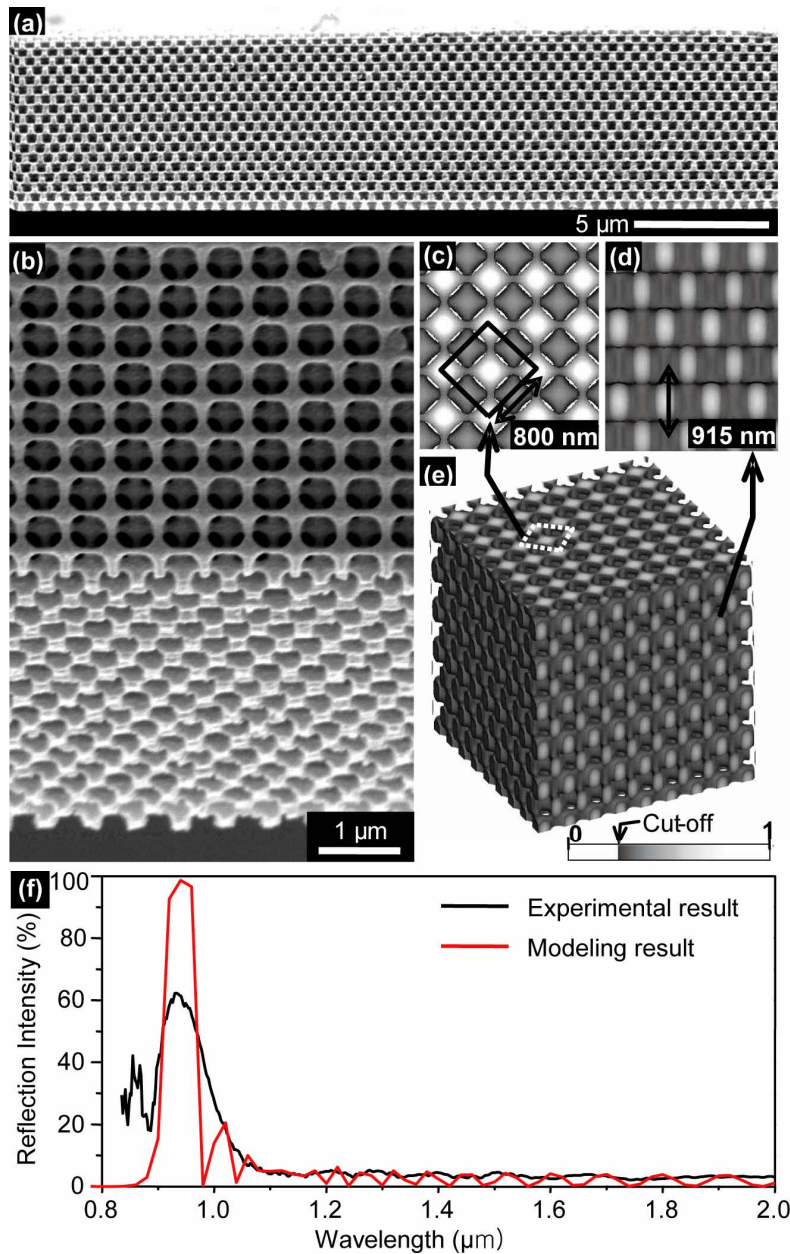


Fig. 3. Scanning electron micrographs of 3D nanostructures formed by 2 photon patterning by exposure through a layer of the photopolymer SU-8 molded with Mask 2. Scanning electron micrograph of cross-sectional (a) and angled (b) views. Intensity distributions computed along the $6(001)$ plane, top view (c), the (110) plane, side view (d), 3D rendering after applying cut-off filter (e), and reflection spectrum from experimental and modeling results (f).

The calculations were performed using Rigorous Coupled Wave Analysis (RCWA) technique [23]. RCWA employs Fourier series expansions to express and approximate unknown electromagnetic fields in order to solve Maxwell's equations for a given frequency on a grating-like structure, which is assumed to be infinitely periodic in transverse directions. Solving Maxwell's equations inside and outside the grating, a matrix representation known as an *S matrix* is produced for the grating. Using the *S matrix*, it is possible to calculate the reflection, transmission and absorption coefficients for the selected frequency. Complex,

three-dimensional structures are divided into grating-like layers in the propagation direction. The S matrices for those layers are then combined to give an overall S matrix for the complex structure. For this experiment we modeled our structure as interconnected cubes arranged in a face centered tetragonal (FCT) lattice with a lattice constant of 566 nm in the transverse directions. The cubes are interconnected with SU8 rods of 100 nm width. The tetragonal lattice pitch in the propagation direction is 800 nm, the cube widths are 350 nm and 32 periods of the FCT lattice were placed along the propagation direction. The discrepancy between the modeling parameters and the parameters implied by the intensity distribution (915 nm pitch, 400 nm cube width) stems from structure shrinkage in post-processing. Experimental measurements were carried out by Fourier Transform Infrared Spectroscopy (Bruker Optics Inc., model Hyperion 1000) with wavelength ranging from 0.8 μm to 2 μm . The spot size in all measurements was 30 nm. The location of peak agrees well, after considering structural shrinkage along the thickness of the structure and variation of filling fraction by exposure time of samples. The shrinkage along the depth of film ranges from ~ 10 to 20% depending on the exposure dose. In-plane periodicity is fixed by the underlying adhesion layer and the shrinkage is negligible in this direction. The magnitude of the reflection peak evaluated by modeling ($\sim 100\%$) is somewhat different than that measured experimentally ($\sim 60\%$). We speculate that the discrepancy between the modeling and measurement arises mostly from irregular shrinkage, surface roughness and other relatively minor structural defects caused during development and drying. The modeling considers, by contrast, idealized structures. In addition, non-uniformities associated with the Gaussian profile of the exposure beam can lead to slight variations in the filling fraction across the measured area. Tighter control over the exposure parameters, and improved mechanical stability in the photopolymer are likely to improve the experimental results.

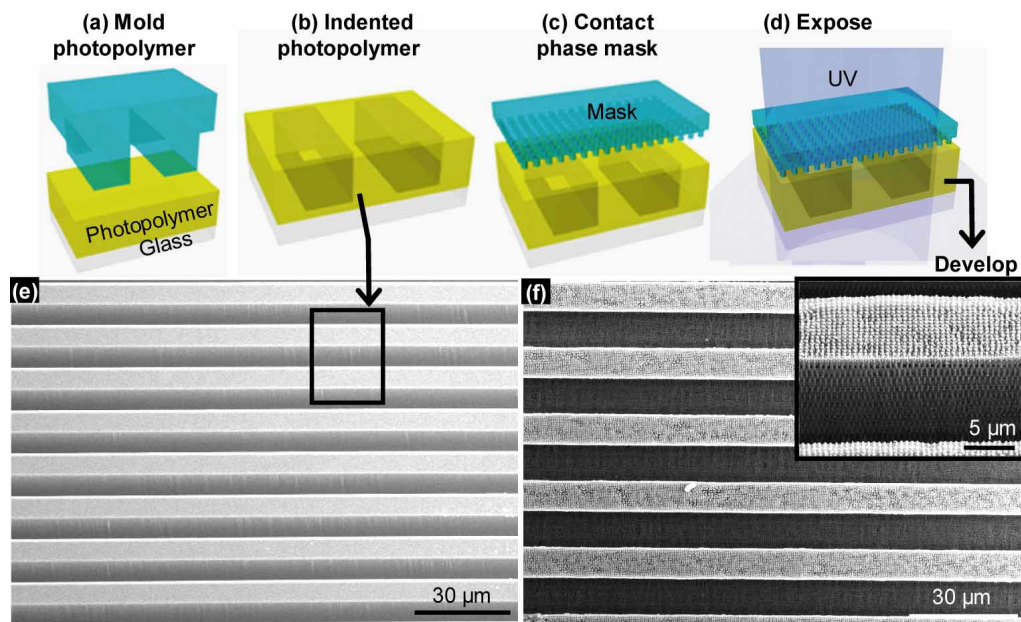


Fig. 4. Schematic illustration of 3D structures formed by first molding coarse ($\sim 10\ \mu\text{m}$ widths and depths) features into a layer of a transparent photopolymer (SU-8) (a,b) and then exposing the structure by passing light through a phase mask while it is in conformal contact with the molded SU-8 (c,d). The scanning electron micrographs show the molded features (e) and the resulting 3D structures (f). The mold for (c) had $10\ \mu\text{m}$ line and space features with relief depth of $10\ \mu\text{m}$. Mask 2 was used for steps (c,d).

Figure 4 demonstrates a second means to exploit molding in 3D optical fabrication. Here, a PDMS mold (mask 4) with coarse structures of relief first molded a layer of SU8 into the form of rib type waveguides with heights and widths of $\sim 10\ \mu\text{m}$. Next, placing mask 2 into

contact with this structure established conformal contact to the raised regions. A blanket exposure through the mask in this configuration exposed the molded waveguides to the 3D distribution of intensity that formed in proximity to the mask and constructed, after postexposure baking and developing, 3D nanostructured waveguides as illustrated in Fig. 4. The coarse relief structures have, of course, some role also in the optics of this process. Index matching fluids could be implemented to avoid such effects, if necessary. Structures of this type could be useful as scattering elements or filled nanoporous elements integrated into optical waveguides, or as semi-permeable boundaries between microfluidic channels.

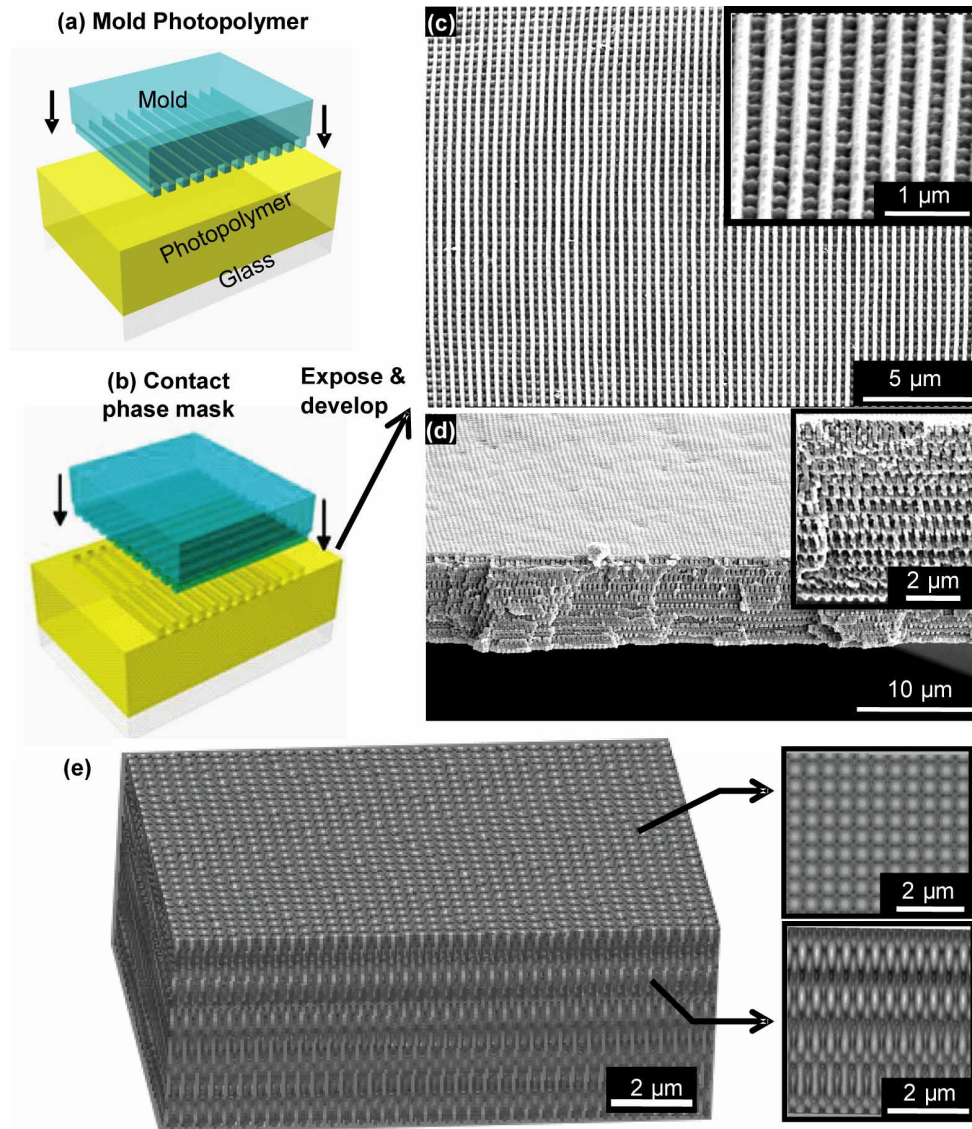


Fig. 5. Schematic illustration of molding mask 3 on SU-8 surface (a) and initiating conformal contact of the same mask on the molded surface (b). SEMs of patterned 3D structures from the system shows top image (c) and bird's eye view (d). Image of modeling from (001) plane, top view (c), from (110) plane, side view (d), and 3D rendering after applying cut-off filter (e). All structures and modeling are from molded SU-8 film by Mask 3.

A third implementation of molding involves the combined use of maskless structures with masks to achieve multi-level phase modulations in geometries that can be much more

complex than either those associated with the molded structures or the masks themselves. As a simple example, illustrated in Fig. 5(a), surface relief structures of line and space phase grating (mask 3) were first molded on the surface of a layer of SU-8. The same PDMS element used for this molding formed the phase mask. Exposing the molded structure through the mask, in conformal contact with its relief structures oriented at 90 degrees relative to the molded ones, yielded an effective 2 level phase modulation in a log pile type configuration [Fig. 5(b)] with maximum phase modulation that is substantially larger than that associated with either the mask or the molded maskless structure. For the mask dimensions used in this demonstration, only nine Fourier components are involved in formation of interference patterns formed with 355 nm exposure light. As in the case of the FCC structure, at the small dimensions associated with mask 3, it is extremely difficult to achieve relief depths that reach the π -phase shift condition, particularly in the case of grating layouts where collapse of adjacent lines is a dominant mechanism for the formation of defects. Mask 3 has a relief depth of ~ 220 nm relief depth which is $\sim \pi/2$ for 355 nm light, such that the combined mask/maskless multi-level grating creates a maximum phase shift that is close to π . Figures 5(c) and 5(d) present images of 3D structures that have 400 nm in plane periodicity. This structure can be interpreted as a superposition of two body centered tetragonal structures that have same in-plane (400 nm) and different out-of-plane (1380 and 2880) lattice parameters. The bottom frames provide modeling results that capture many aspects of these structures.

4. Conclusion

In summary, this paper introduces a method for combining molding, or nanoimprint, techniques with phase mask approaches to fabricate 3D structures in transparent photosensitive materials. These ideas provide additional design flexibility in the structure geometries that can be achieved compared to those possible with optical approaches alone, due either to limitations associated with the optics and/or materials used for the phase masks. Examples presented here illustrate, in particular, the ability to form structures with geometries approaching FCC, with both coarse and fine features and with log pile-like layouts. Addition of amplitude modulating elements, mask designs with increased complexity and other strategies might be implemented in conjunction with the molding techniques presented here to enable further advances in this type of patterning technology.

Acknowledgment

This work is supported by DOE-LLNL through grant B529271, DOE rant No. DEFG02-91ER45439, NSF through grant DMI 03-55532 and DMR-0415187. Frederick Seitz Materials Research Laboratory, University of Illinois, which is partially supported by the U.S. Department of Energy under grant DEFG02-91-ER45439 and Sandia National Laboratories, a multiprogram laboratory operated by Sandia Corporation, a Lockheed Martin Company, for the U.S. Department of Energy's National Nuclear Security Administration under contract DE-AC04-94AL85000. Use of the Center for Nanoscale Materials was supported by the U. S. Department of Energy, Office of Science, Office of Basic Energy Sciences, under Contract No. W-31-109-Eng-38.